Valley splitting and optical intersubband transitions at parallel and normal incidence in [001]-Ge/SiGe quantum wells

Michele Virgilio and Giuseppe Grosso
Dipartimento di Fisica "E. Fermi" and NEST-INFM, Universitsità di Pisa, Largo Pontecorvo 3, I-56127 Pisa, Italy
(Received 14 January 2009; published 15 April 2009)

We investigate intervalley splitting in the conduction band of strained [001]-Ge quantum well (QW) systems with finite SiGe alloy barriers by means of a $sp^3d^5s^*$ tight-binding Hamiltonian. We find that interaction between germanium bulk L minima splits each confined subband into a doublet. We first characterize this splitting as a function of the well width and of the strength of a uniform electric field superimposed along the growth direction. Varying the well width, an oscillating behavior of the splitting magnitude similar to that predicted for Si QW systems is observed and explained. Then we focus on the optical intersubband transitions occurring between states belonging to the fundamental and the first-excited doublets. Selection rules for intersubband transitions at normal and parallel incidence are discussed exploiting the parity character of the involved doublet states. Numerical results for infrared-absorption spectra, evaluated for both symmetric and biased Ge QWs, support our findings.

DOI: 10.1103/PhysRevB.79.165310 PACS number(s): 73.21.Fg, 78.67.De

I. INTRODUCTION

Conduction electronic states in low dimensional semiconductor systems based on indirect-gap materials may display a doublet structure at the meV scale. This energy separation, known as intervalley splitting (IS), is caused by the interaction of the confined states belonging to conjugated valley minima with nonvanishing component of the $\vec{k}$ vector along the confinement direction. For instance in a [001] tensile strained silicon layer, the bottom conduction doublet results from the interaction of the two confined states which originate from the Δ valleys along the [001] and $[00\bar{1}]$ directions.

Originally IS was studied theoretically[1–3] and demonstrated experimentally[4] in [001]-silicon inversion layers. However intervalley coupling is quite a general feature which is observed in two-dimensional (2D),[5] one-dimensional,[6] or zero-dimensional[7–9] systems in the indirect-gap regime, as for instance GaSb/AlSb,[10,11] $GaAs/Al_xGa_{1-x}As$ with high Al concentration,[12] or SiGe (Refs. 7, 9, and 13–26) alloys.

From the experimental side IS was deeply investigated by means of magnetotransport measurements, mainly in 2D Si-based systems.[4,5,9,12,13,20,21,27,28] From the theoretical side intervalley coupling in 2D systems was early studied in the framework of the multivalley envelope function effective-mass model[1–3] and by means of the one-band Wannier orbital model.[11] More recently it has been addressed within an atomistic framework by means of two orbital and multiorbital tight-binding (TB) models,[14,17,19,22,26,29] and conceptual and quantitative connection with the effective-mass description provided.[10,15,16,22–24] As well, also the pseudopotential method versus the effective-mass model was adopted for the study of intervalley splitting.[25]

The increasing interest toward IS in Si and SiGe systems is mainly motivated by the need to achieve simultaneous control of both valley[7–9,13,14,17–24,26–28] and spin[15,16,30,31] degrees of freedom. This would permit selective population of the lowest conduction doublet which is crucial for silicon-based spintronics and quantum computing applications.[32]

As recently demonstrated in Refs. 25, 33, and 34, IS is expected to play a role also in optical applications; in fact it influences the intersubband optical absorption of n-type indirect-gap systems as SiGe Multiple Quantum Wells (MQWs) or SiGe quantum cascade structures. As clarified in the following, the influence of IS on the intersubband absorption spectrum can be interpreted in terms of selection rules which stem from the different spatial parities of the electronic states within each valley-split subband.

In the study of IS in biaxially strained [001]-SiGe two-dimensional systems, one has to distinguish the case of low and high Ge contents of the active region. If the fractional Ge content is lower than ~0.85, the conduction minima are located at about 0.83% of the Γ-X segment along the Δ_2 or Δ_4 lines for tensile or compressive in-plane strain, respectively. For high Ge content, the conduction minima of the constituting bulk materials are at the L point of the Brillouin zone (BZ). In this case, under a [001]-biaxial strain field the $\langle 111\rangle$ directions remain equivalent and the L point degeneracy is preserved. Therefore in [001]-grown Ge-rich strained heterostructures, the intervalley interaction involves the four couples of L states each couple of the conjugated valleys giving rise to valley-split doublets.

In the present paper we focus on IS and intersubband absorption between valley-split subbands in strained Ge/SiGe QW structures. We stress that despite Ge-rich heterostructures having been insofar poorly investigated, mainly because of the difficulties of growing coherent multilayer samples,[35] they display a number of peculiar properties relevant for optoelectronic applications.[36] Indeed, only very recently high quality Ge-rich SiGe heterostructures have become available thanks to new advances in SiGe epitaxy.[37,38]

For what concerns conduction intersubband transitions in Ge-rich systems, we notice that the possibility of achieving robust confinement potential at the L point was predicted by a number of independent works[39–41] while demonstration of significant conduction confinement potential in low-Ge content heterostructures remains elusive. Moreover due to the light effective mass at the L point, n-type Ge-rich multilayer

 ©2009 The American Physical Society

systems have been indicated as most promising candidates in the run to silicon integrable Quantum Cascade Laser (QCL).[42]

Finally, it is worth mentioning that, in Ge-rich [001]-multilayer structures, intersubband transitions can be stimulated both in TE and TM modes of the incident radiation.[43] This fact is due to the presence of off-diagonal terms in the mass tensor at the L point (the constant energy ellipsoids have principal axes along the $\langle 111\rangle$ directions while the considered systems are grown along the [001] direction) which guarantees coupling between electronic states and radiating fields of arbitrary polarization. We exploit this possibility to suggest experimental arrangements for optical detection of IS.

The paper is organized as follows. In Sec. II we present our tight-binding results for the IS in Ge/SiGe quantum wells as a function of the QW width and of a uniform electric field superimposed to the system along the growth direction. The spatial parities of the confined states, investigated by orbital and layer projections, are also discussed. In Sec. III intersubband absorption between valley-split subbands obtained for different values of QW widths, doping concentrations, and electric fields are presented. We demonstrate that the different magnitude of the IS in the fundamental and first-excited double, and the selection rules stemming from the spatial parities of the valley-split states can be responsible for observable features in the absorption spectrum. Our conclusions are reported in Sec. IV.

II. TIGHT-BINDING CONDUCTION BAND VALLEY SPLIT STRUCTURE OF GE/SIGE QUANTUM WELLS

The essential physical picture of valley splitting which emerges from the above quoted multivalley effective-mass analytic results and TB numerical simulations is well understood as due to the confinement potential at the heterointerfaces, which produces a coupling between the conjugated valleys. In particular, for a symmetric square well it has been found that QW states can be described in terms of symmetric or antisymmetric combinations of the bulk states associated with the two conjugated conduction valleys. Each IS doublet is composed by a symmetric and an antisymmetric confined state wave function characterized by the same envelope function. The valley coupling is governed by a mixing potential localized at the heterointerfaces whose strength is an oscillating function of the well width L_W and valley distance Δk. It follows that also the amplitude of the IS splitting, ΔE, oscillates according to the relation $\Delta E \propto \sin(\Delta k L_W/2)$.[11] Moreover, since the mixing potential is localized at the heterointerfaces, ΔE is also proportional to the square amplitude of the confined wave functions at the well boundaries.[24] Therefore IS is also a decaying function of the well width with a power-law exponent equal to -2.6 (Ref. 11) or -3 (Ref. 17). We show numerically that this behavior is also found for the conduction-band states confined at the L point in the considered Ge/SiGe QWs.

The QW systems investigated in this paper are composed of compressively strained Ge QWs sandwiched by tensile

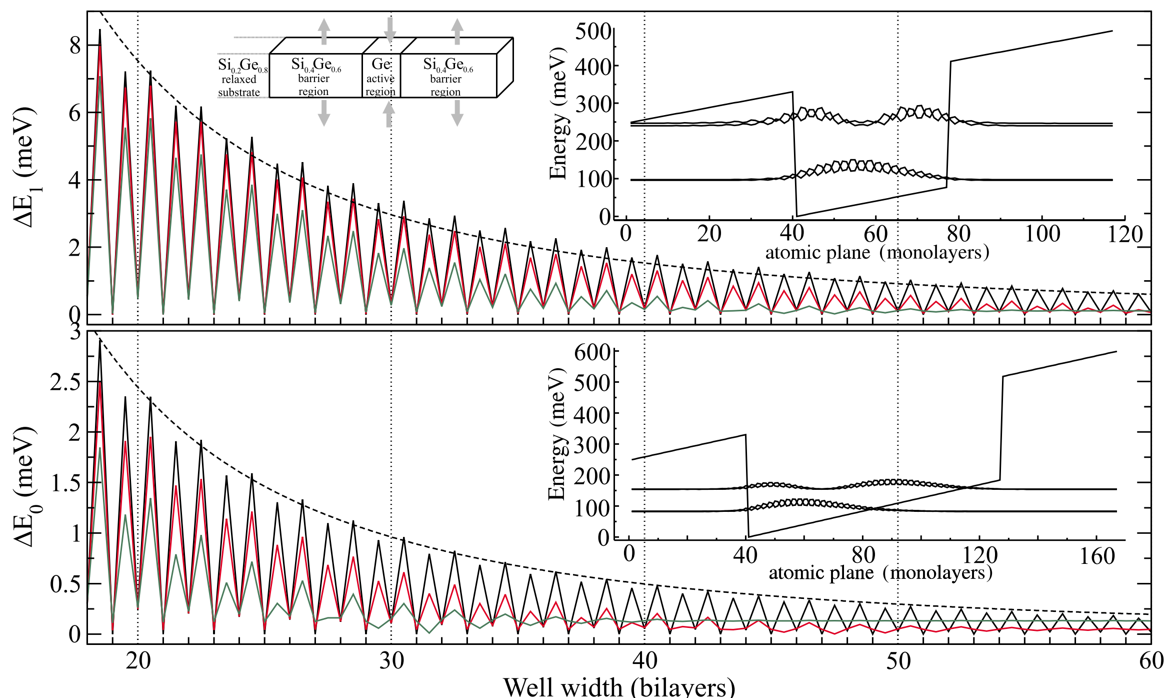

FIG. 1. (Color online) Valley splitting magnitude versus well width (number of bilayers in the active region) for the ground (E_0 level, bottom panel) and first-excited (E_1 level, top panel) QW subbands. Each bilayer is composed of two Ge atomic layers in the anion and cation positions. Solid black, red, and green lines refer to $\mathcal{E}$ equal to 0, 5, and 15 mV/Å, respectively. Black dashed lines represent the best fits obtained by means of the analytic expression discussed in the text. Ge concentrations in the buffer, barrier, and well regions are reported in the top panel (gray arrows indicate the direction of the in-plane strain fields). QW band-edge profiles at $\mathcal{E}=15$ mV/Å together with the square modulus of the wave functions for the E_0 and E_1 doublets are sketched in the insets; the top (bottom) inset refers to a QW system with well width of 37 (87) monolayers.

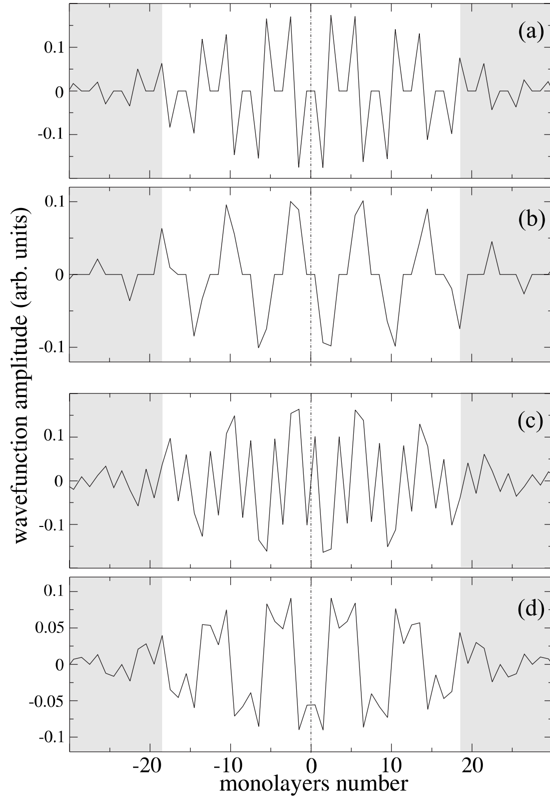

FIG. 2. Wave function amplitude at zero electric field of the even ($E_0^{(1)}$) and of the odd ($E_0^{(2)}$) states, belonging to the ground doublet of the Ge QW system. The well is composed of 37 monoatomic layers, corresponding to a maximum in the valley-splitting amplitude. Shaded gray area indicates the barrier regions. Plots (a) and (b) represent the contribution to the wave-function amplitude of the $E_0^{(1)}$ state obtained from orbitals which are even and odd under the $\hat{z} \to -\hat{z}$ transformation, respectively. Plots (c) and (d) refer to the even and odd orbital contributions to the $E_0^{(2)}$ wave function, respectively.

strained $Si_{0.4}Ge_{0.6}$ barriers, coherently grown along the [001] direction on a relaxed $Si_{0.2}Ge_{0.8}$ substrate. In the well material the bottom of the conduction band is located at the L point and the barrier height resulting from the band-edge profile is $\simeq 330$ meV. This value is similar to those usually derived for strained Si/SiGe QWs with low-Ge content in the barriers.[17,33]

The equilibrium positions of the ions are evaluated by means of elasticity theory as discussed in Ref. 33. Heterointerfaces are assumed sharp and the barrier thickness is chosen so to ensure that the wave functions for the confined QW states are extinguished well before the boundaries of the well+barrier system. In this condition periodic or hard wall boundary conditions along the [001] direction can be equivalently chosen. Periodic boundary conditions are exploited in the growth plane. Electronic states are described by means of a first neighbors $sp^3d^5s^*$ TB Hamiltonian including spin-orbit interaction. We have adopted the self and hopping energy parameters derived semiempirically by Jancu *et al.*[44] for bulk silicon and germanium crystals. Since Si and Ge are miscible in the whole composition range, alloying in the barriers is treated within the virtual-crystal approximation (VCA), interpolating linearly with Ge concentration the parameters of Ref. 44. A recent discussion of such approximation in the TB framework can be found in Ref. 45. Effects of strain in the barrier and well regions are accounted for by suitable scaling laws for the hopping parameters.[44] The near gap confining potential along the growth direction is inserted in the model adding a constant term to the site-diagonal energy parameters of the Hamiltonian in the barrier region. Its value is chosen so as to reproduce the valence-band offsets derived in Ref. 46. As well, uniform electric fields superimposed along the growth direction are modeled as diagonal z-dependent contributions to the Hamiltonian.

In Fig. 1 is reported the evaluated energy difference $\Delta E_0 = |E_0^{(1)} - E_0^{(2)}|$ $(\Delta E_1 = |E_1^{(1)} - E_1^{(2)}|)$ at the L point between the lowest conduction levels corresponding to the fundamental (first-excited) doublet, as a function of the number of biatomic layers in the well region (solid black line). A power-law fit $|\Delta E_i| \propto L_W^{-\gamma}$ with $\gamma = 2.3$ well reproduces the damping of the oscillations of ΔE_0 and ΔE_1 with the well width (dashed black line). This value is of the same order as those reported for silicon QW systems $\gamma = 2.6$ (Ref. 11) or $\gamma = 3$ (Ref. 17). Indeed the IS oscillations reported in Fig. 1 closely resemble IS oscillations of Si QWs.[17,33] For instance also in Si QW systems the oscillations of the splitting energies for the fundamental and excited doublets have a common period and phase. Moreover, in agreement with envelope function models it holds $\Delta E_1 > \Delta E_0$ due to the larger value of the wave function for the first-excited levels at the well boundaries where the mixing heterointerface potential is active. Nevertheless, two relevant differences are worth to be stressed. First, for [001]-Ge QWs we find IS values larger than the corresponding values of [001]-Si QWs. As an example, we get for a 37 Ge monolayer QW $\Delta E_0 = 2.9$ meV and $\Delta E_1 = 8.5$ meV (see Fig. 1). These quantities are to be compared with $\Delta E_0 = 1.3$ meV and $\Delta E_1 = 5.4$ meV obtained for a [001]-Si QW with the same width, by means of the same TB model.[33] Since also the barrier height of the confining potentials of the Si QW studied in Ref. 33 are approximately the same as for the Ge QW here studied, the larger IS splittings we find for the Ge QWs are due to the L point quantization effective mass which is lighter than the longitudinal Δ mass of silicon [see Eq. (25) in Ref. 24].

The second relevant difference with respect to Si QW systems concerns the period of the IS oscillations. In the case of [001]-Si QWs the distance Δk between the two interacting valleys (each located at about 0.83% of the Γ-X segment) leads to an oscillation period for $|\Delta E_i|$ of about 6.4 bilayers. This value is larger than the period of 1 bilayer that we obtain in the case of Ge QWs (see Fig. 1). Our result for the IS period is in agreement with Ref. 11 where intervalley coupling between the L minima in GaSb/AlSb QW and SL systems was studied both with a $\vec{k} \cdot \vec{p}$ envelope function and a one-band Wannier orbital model.

We notice that, since in the present paper heterointerfaces are assumed abrupt and flat, the values reported in Fig. 1 exactly hold in the theoretical limit of perfect interfaces while the inclusion of interface disorder should not affect them dramatically.[19,25]

A superimposed electric field $\vec{\mathcal{E}}$ along the $\hat{z}$ direction breaks the QW symmetry; thus a destructive effect on the IS

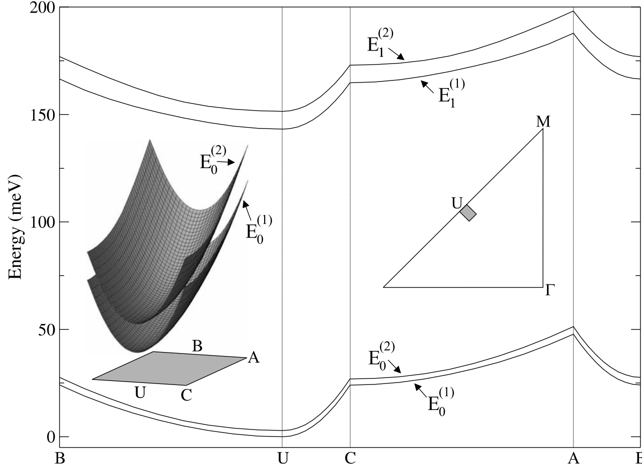

FIG. 3. Band dispersion at zero field in the growth plane for the E_0 and E_1 doublets, evaluated along the path reported in the insets. In the tetragonal Brillouin-zone description adopted here, the U point corresponds to the conduction minimum of the strained Ge bulk crystal (L point) and the Γ-M segment to the Δ line. The small gray rectangle (right inset) indicates the part of the BZ that was sampled to evaluate the intersubband absorption spectrum. In the left inset the same rectangle is reported together with the corresponding $E_0^{(1)}$ and $E_0^{(2)}$ energy surfaces.

oscillations is expected.[24,33] However we observe that for moderate fields the IS oscillations are still observable, with unchanged period and phase (red and green curves in Fig. 1). For a given electric-field strength the IS oscillations are destroyed only for large enough wells. Moreover IS oscillations in the E_1 doublet survive for higher fields with respect to the E_0 doublet. These behaviors can be understood by analyzing the effect of the electric field on the confined wave functions (see insets of Fig. 1). For moderate fields both the E_0 and E_1 wave functions contact the right wall of the QW as shown in the top inset of Fig. 1. A proper increase in the electric field can cause the vanishing of the E_0 and E_1 wave functions at the right side of the well. This is shown in the bottom inset of Fig. 1. Only in this condition the triangular shaped potential originated by the field prevents the interference of the doublet wave functions originated by multiple reflections at the QW walls and the IS splitting becomes independent from the QW width. The same effect was numerically observed also in [001]-Si QW systems.[24,26,33,47] In that case, because of the lower confinement energy due to the heavy longitudinal Δ mass, weaker electric fields are sufficient to destroy IS oscillations.[24,33]

Wave functions belonging to the same doublet share the same envelope function[24] but are characterized by atomic scale oscillation with opposite phases;[33] this guarantees that, for symmetric QW, the two levels in each doublet have opposite parity. An accurate analysis of the group symmetry of SiGe QWs as function of the number of monoatomic layers in the QW region can be found in Refs. 15 and 31. Opposite phases within each doublet are evident in the insets of Fig. 1. A more detailed description of the doublet wave-function oscillations is shown in Fig. 2 where we have plotted the amplitude of the wave functions at zero electric field of the (even) $E_0^{(1)}$ and of the (odd) $E_0^{(2)}$ states, belonging to the ground doublet of a 37 monoatomic layer Ge QW. To reveal the spatial parity of the states, the contributions to the wave function from orbitals which are even or odd with respect to the $\hat{z}\rightarrow-\hat{z}$ transformation have been separated. For instance the even $E_0^{(1)}$ state is characterized by the even (odd) component of the wave function associated to $\{s,s^*,p_x,p_y,d_{xy},d_{x^2-r^2},d_{3z^2-r^2}\}(\{p_z,d_{yz},d_{zx}\})$ orbitals.

III. ABSORPTION SPECTRUM AND SELECTION RULES FOR INTERSUBBAND VALLEY SPLIT TRANSITIONS IN GE/SIGE QWS

We now focus on intersubband transitions in ultrathin symmetric Ge QW systems between the valley-split E_0 and E_1 doublets. Intersubband absorption is evaluated sampling the BZ in a suitable neighbor of the $L\equiv U$ point to include all the $\vec{k}$ vertical transitions active in a given energy range. The absorption coefficient $\alpha(\hbar\omega)$ for incident light with polarization unit vector $\hat{\epsilon}$ and energy $\hbar\omega$ is calculated according to

$$\alpha(\hbar\omega)=\frac{2\pi e^2\hbar}{n_0 c m_0 V\Gamma}\sum_{\vec{k}}\sum_{i,j}\frac{P^{\epsilon}_{i,j}(\vec{k})}{E_i(\vec{k})-E_j(\vec{k})}\cdot\{f[E_j(\vec{k})] - f[E_i(\vec{k})]\}\cdot\frac{1}{1+\left(\frac{E_i-E_j-\hbar\omega}{\Gamma}\right)^2}, \quad (1)$$

where $P^{\epsilon}_{i,j}(\vec{k})=(2/m_0)|\langle i,\vec{k}|\hat{\epsilon}\cdot\vec{p}|j,\vec{k}\rangle|^2$ is the squared modulus of the dipole matrix element, expressed in electron volts, between conduction intersubband states $|j,\vec{k}\rangle$ and $|i,\vec{k}\rangle$ of energies E_j and E_i, respectively; $f(E)$ is the Fermi distribution function, and n_0 is the refractive index which is assumed independent on frequency in the energy range of interest. Line broadening effects are phenomenologically included in Eq. (1) substituting the delta function with a Lorentzian distribution of linewidth $\Gamma=1$ meV. More details on the evaluation of optical properties in the semiempirical tight-binding framework can be found in Ref. 33.

We have numerically shown in Sec. II that ΔE_1 is larger than ΔE_0, and then in principle four different transitions, nondegenerate at the meV scale, are possible. However for selected polarization vectors, only a subset of these transitions is allowed because of the different spatial parities of the involved states.[33] Consider first the polarization vector of the incident radiation along the growth ($\hat{z}$) axis which corresponds to incidence parallel to the QW plane. This is the standard configuration used to couple the radiating field to the electronic subband levels in n-type QW systems. In this case the dipole operator is odd with respect to the $\hat{z}\rightarrow-\hat{z}$ transformation and only intersubband transitions between states with opposite parities are allowed. On the contrary, if the radiating field propagates normally to the QW plane, the dipole operator is even and only states with the same spatial parity can be coupled by the electromagnetic field. Moreover, we observe that in Si-rich [001]-SiGe QWs the lowest conduction states (Δ_2) are mainly composed of s, $s*$, p_z, and d_{xy} orbitals. With light propagating along the QW axis the electric field lies in the x-y plane, and without any appreciable p_x, p_y or d_{zx}, d_{yz} components there is no way it can

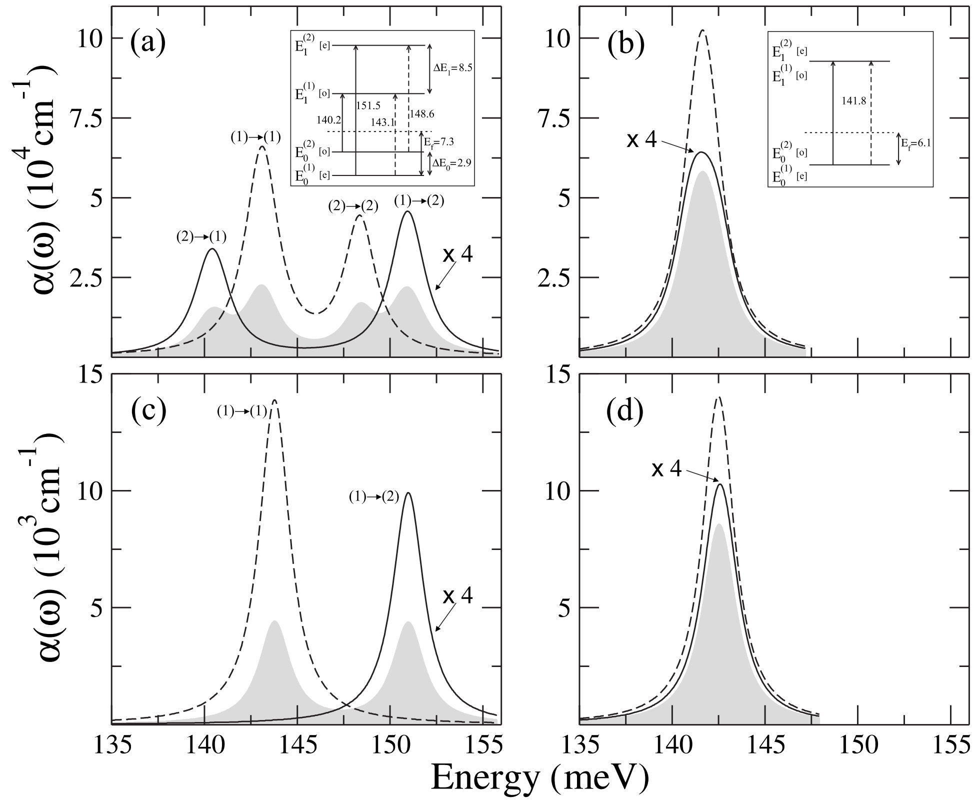

FIG. 4. Low temperature intersubband absorption spectra evaluated at $\mathcal{E}=0$ for normal (solid lines) and parallel (dashed lines) incident radiations. Left (right) plots refer to a 37 (38) monolayer QW systems, corresponding to a maximum (minimum) of the valley-splitting oscillation. Grey shaded features represent the joint density of states and the normal-incidence absorption is reported magnified by four. For the (a) and (b) plots, carrier concentration per layer in the well region is 8×10^{-6} Å^{-2}. The related $T=0$ Fermi energies and level diagrams are shown in the insets; parity of the states and allowed transitions for both polarizations (solid and dashed arrows) are also indicated. (c) and (d) panels refer to a carrier concentration of 1×10^{-6} Å^{-2}; in this case, E_f for the 37 monolayer QW system [(c) panel] is equal to 1.54 meV and only the $E_0^{(1)}$ subband is populated.

couple states in the QW. In contrast, in Ge-rich [001]-SiGe QWs the lowest conduction states near the L point have essentially equal p_x, p_y, and p_z components, and electric-dipole transitions are allowed. From the effective-mass perspective, the same conclusions follow observing that, in Si-rich [001]-SiGe QWs, normal incident radiation does not stimulate conduction intersubband transitions because the electric field oscillates in the QW plane which is a free direction for the motion of the Δ electrons; in Ge-rich [001]-SiGe QWs, the in-plane field is coupled to the motion along the confined direction by the off-diagonal terms of the mass tensor at L.[43]

To evidence the effect of these selection rules on the intersubband absorption spectrum, we have evaluated $\alpha(\omega)$ in n-type QW systems with different values of the doping concentrations and QW widths, both in the presence and in the absence of electric fields superimposed along the growth direction. For the investigated doping concentrations ($n^+=10^{-6}-10^{-5}$ Å^{-2}) and in the low-temperature regime, only electronic states in a small neighbor of the U point are populated and the sampling of the quasi-2D BZ can be reduced to the gray shaded region depicted in Fig. 3. It is useful to note that the ΔE_0 and ΔE_1 splittings remain almost constant for all the $\vec{k}$ points belonging to this region (see Fig. 3). This happens because the extension of the sampled region is very small with respect to the BZ and then the magnitude of the mixing potential which governs the amplitude of the IS is almost constant there.[11]

In Fig. 4 we show the low-temperature intersubband absorption spectra evaluated at the field $\mathcal{E}=0$ for 37 (left panels) and 38 (right panels) monolayer Ge QWs. These QW widths correspond to a maximum and a minimum of the IS, respectively (see Fig. 1). Panels (a) and (b) refer to a doping concentration in the well region of 8×10^{-6} Å^{-2}. For this doping value we obtain $E_f=7.3$ meV and $E_f=6.1$ meV, respectively (see top insets of Fig. 4). Let us examine first panel (a). Both the $E_0^{(1)}$ and $E_0^{(2)}$ levels are populated and then four different transitions can be observed as evidenced from the gray shaded region which represents the $E_0^{(i)}\rightarrow E_1^{(j)}$ joint density of states. In agreement with the above considerations, we found that for polarization vector along the growth axis only two peaks are present in the absorption spectrum (dashed line). These peaks correspond to the $E_0^{(1)}\rightarrow E_1^{(1)}$ and the $E_0^{(2)}\rightarrow E_1^{(2)}$ transitions which involve even and odd states, respectively. On the contrary, only transitions between states with the same parity, i.e., $E_0^{(1)}\rightarrow E_1^{(2)}$ and the $E_0^{(2)}\rightarrow E_1^{(1)}$, are observed when the polarization vector is chosen in the QW plane (solid line). The spectra reported in panel (b) are instead characterized by a single peak whose energy does not depend on the polarization vector. This is an immediate consequence of the absence of IS in both the E_0 and E_1 doublets.

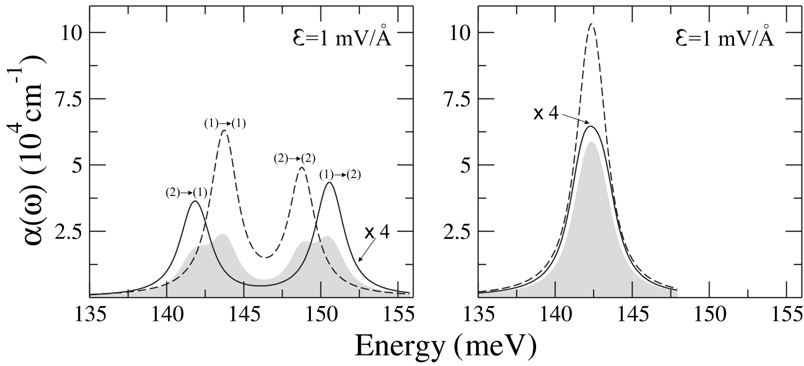

FIG. 5. Low temperature intersubband absorption spectra at normal (solid lines) and parallel (dashed lines) incident radiations evaluated at $\mathcal{E}=1$ mV/Å for the 37 (left panel) and 38 (right panel) monolayer QW systems. Carrier concentration per layer in the well region is 8×10^{-6} Å^{-2} and E_f is equal to 7 (left panel) and 6.1 meV (right panel); normal-incidence absorption is reported magnified by four.

Panels (c) and (d) have been obtained reducing the doping concentration in the well region to $n^{+}=1\times10^{-6}$ Å^{-2}. Because of the zero IS splitting in the case of 38 monolayer QW, both the $E_0^{(1)}$ and $E_0^{(2)}$ states are still populated [panel (d)]. Therefore the absorption spectra of panels (b) and (d) are similar. A different situation is obtained in the case of the 37 monolayer QW. Carriers are now present only in the ground $E_0^{(1)}$ state ($E_f=1.54<|\Delta E_0|$). As a consequence a single peak whose energy is polarization dependent characterizes the absorption spectrum. For polarization vector in (orthogonal to) the QW plane, the peak is associated to the $E_0^{(1)}\rightarrow E_1^{(2)}$ ($E_0^{(1)}\rightarrow E_1^{(1)}$) transition.

Finally, we have investigated the effect of the electric field on the selection rules discussed above. In principle the breaking of the $\hat{z}\rightarrow-\hat{z}$ symmetry caused by the field should be responsible for a partial transfer of the oscillator strengths toward the previously forbidden transitions. We find instead that the selection rules still hold even when the envelope wave functions become strongly asymmetric. The same result was previously obtained in the contest of [001]-Si QWs,[33,34] and is probably due to the persistence of the atomic scale oscillations in the wave functions whose period and phase result to be unaffected by the electric field (see Ref. 33). Intersubband spectra obtained for the 37 and 38 monolayer width QWs with $\mathcal{E}=1$ mV/Å are shown in Fig. 5.

IV. CONCLUSIONS

By means of a multiorbital tight-binding model we have investigated the intervalley coupling in the conduction band of strained Ge/SiGe QWs grown on [001] Ge-rich substrates. For the chosen Ge contents in the substrate and well materials, the bottom conduction states are located at the L point and we find that the resulting band-edge profile allows a robust confinement of electron states in the Ge active region. The valley splitting of fundamental and first-excited subbands has been studied as a function of the QW width for different values of a static electric field superimposed along the growth direction. In agreement with $\vec{k}\cdot\vec{p}$ effective-mass calculations, we find that also for Ge QWs IS has an oscillating behavior as function of the QW width with a power-law decay. The period of oscillations is governed by the distance in $\vec{k}$ space of the conjugated L minima and then differs from what is predicted for [001]-SiGe QWs with low-Ge content. The spatial parity of the valley-split states has been numerically studied by orbital and layer projections. Selection rules induced by the opposite spatial parity of the states belonging to the same IS doublet have been numerically verified. Their influence on the intersubband absorption spectrum involving the ground and first-excited doublets of n-type systems has been investigated as function of doping concentrations, QW widths, and polarization vector of the incident radiation. Our results suggest that in ultrathin Ge/SiGe QW systems the IS can be responsible for observable features in the absorption spectrum. This fact might be exploited to measure IS by means of optical instead of magnetotransport techniques. Our results are also relevant for the design of SiGe-based quantum cascade emitters and Si-integrable quantum computation or spintronic devices.

ACKNOWLEDGMENT

This work has been supported by National Enterprise for NanoScience and NanoTechnology (NEST).

[1] F. Stern and W. E. Howard, Phys. Rev. **163**, 816 (1967).

[2] L. J. Sham and M. Nakayama, Phys. Rev. B **20**, 734 (1979).

[3] F. J. Ohkawa, Solid State Commun. **26**, 69 (1978).

[4] A. B. Fowler, F. F. Fang, W. E. Howard, and P. J. Stiles, Phys. Rev. Lett. **16**, 901 (1966).

[5] T. Ando, A. B. Fowler, and F. Stern, Rev. Mod. Phys. **54**, 437 (1982).

[6] Y. Zheng, C. Rivas, R. Lake, K. Alam, T. Boykin, and G. Klimeck, IEEE Trans. Electron Devices **52**, 1097 (2005).

[7] S. Srinivasan, G. Klimeck, and L. P. Rokhinson, Appl. Phys. Lett. **93**, 112102 (2008).

[8] D. Ahn, J. Appl. Phys. **98**, 033709 (2005).

[9] L. M. Mcguire, M. Friesen, K. A. Slinker, S. N. Coppersmith, and M. A. Eriksson, arXiv:0810.0538 (unpublished).

[10] J. M. Jancu, R. Scholz, G. C. La Rocca, E. A. de Andrada e Silva, and P. Voisin, Phys. Rev. B **70**, 121306(R) (2004).

[11] D. Z.-Y. Ting and Y. C. Chang, Phys. Rev. B **38**, 3414 (1988).
[12] Y. P. Shkolnikov, E. P. De Poortere, E. Tutuc, and M. Shayegan, Phys. Rev. Lett. **89**, 226805 (2002).
[13] M. A. Wilde, M. Rhode, C. Heyn, D. Heitmann, D. Grundler, U. Zeitler, F. Schäffler, and R. J. Haug, Phys. Rev. B **72**, 165429 (2005).
[14] T. B. Boykin, N. Kharche, and G. Klimeck, Phys. Rev. B **77**, 245320 (2008).
[15] M. O. Nestoklon, L. E. Golub, and E. L. Ivchenko, Phys. Rev. B **73**, 235334 (2006).
[16] M. O. Nestoklon, E. L. Ivchenko, J.-M. Jancu, and P. Voisin, Phys. Rev. B **77**, 155328 (2008).
[17] T. B. Boykin, G. Klimeck, M. Friesen, S. N. Coppersmith, P. von Allmen, F. Oyafuso, and S. Lee, Phys. Rev. B **70**, 165325 (2004).
[18] J.-C. Chiang, Jpn. J. Appl. Phys., Part 1 **33**, L294 (1994).
[19] N. Kharche, M. Prada, T. B. Boykin, and G. Klimeck, Appl. Phys. Lett. **90**, 092109 (2007).
[20] K. Lai, T. M. Lu, W. Pan, D. C. Tsui, S. Lyon, J. Liu, Y. H. Xie, M. Muhlberger, and F. Schaffler, Phys. Rev. B **73**, 161301(R) (2006).
[21] S. Goswami *et al.*, Nat. Phys. **3**, 41 (2007).
[22] S. Lee and P. von Allmen, Phys. Rev. B **74**, 245302 (2006).
[23] M. Friesen, M. A. Eriksson, and S. N. Coppersmith, Appl. Phys. Lett. **89**, 202106 (2006).
[24] M. Friesen, S. Chutia, C. Tahan, and S. N. Coppersmith, Phys. Rev. B **75**, 115318 (2007).
[25] A. Valavanis, Z. Ikonić, and R. W. Kelsall, Phys. Rev. B **75**, 205332 (2007).
[26] T. B. Boykin, G. Klimeck, M. A. Eriksson, M. Friesen, S. N. Coppersmith, P. von Allmen, F. Oyafuso, and S. Lee, Appl. Phys. Lett. **84**, 115 (2004).
[27] K. Lai, W. Pan, D. C. Tsui, S. Lyon, M. Mühlberger, and F. Schäffler, Phys. Rev. Lett. **96**, 076805 (2006).
[28] K. Takashina, Y. Ono, A. Fujiwara, Y. Takahashi, and Y. Hirayama, Phys. Rev. Lett. **96**, 236801 (2006).
[29] G. Grosso, G. Pastori Parravicini, and C. Piermarocchi, Phys. Rev. B **54**, 16393 (1996).
[30] A. M. Tyryshkin, S. A. Lyon, W. Jantsch, and F. Schäffler, Phys. Rev. Lett. **94**, 126802 (2005).
[31] L. E. Golub and E. L. Ivchenko, Phys. Rev. B **69**, 115333 (2004).
[32] S. A. Wolf, D. D. Awschalom, R. A. Buhrman, J. M. Daughton, S. von Molnar, M. L. Roukes, A. Y. Chtchelkanova, and D. M. Treger, Science **294**, 1488 (2001).
[33] M. Virgilio and G. Grosso, Phys. Rev. B **75**, 235428 (2007).
[34] M. Virgilio and G. Grosso, Physica E (Amsterdam) **40**, 2046 (2008).
[35] K. Brunner, Rep. Prog. Phys. **65**, 27 (2002).
[36] R. Soref, IEEE J. Sel. Top. Quantum Electron. **12**, 1678 (2006).
[37] G. Isella, D. Chrastina, B. Rössner, T. Hackbarth, H. J. Herzog, U. König, and H. von Känel, Solid-State Electron. **48**, 1317 (2004).
[38] M. Bonfanti, E. Grilli, M. Guzzi, M. Virgilio, G. Grosso, D. Chrastina, G. Isella, H. von Kanel, and A. Neels, Phys. Rev. B **78**, 041407(R) (2008).
[39] M. M. Rieger and P. Vogl, Phys. Rev. B **48**, 14276 (1993).
[40] F. Schäffler, Semicond. Sci. Technol. **12**, 1515 (1997).
[41] M. Virgilio and G. Grosso, J. Phys.: Condens. Matter **18**, 1021 (2006).
[42] L. Lever, A. Valavanis, Z. Ikonić, and R. W. Kelsall, Appl. Phys. Lett. **92**, 021124 (2008).
[43] M. Virgilio and G. Grosso, Nanotechnology **18**, 075402 (2007).
[44] J.-M. Jancu, R. Scholz, F. Beltram, and F. Bassani, Phys. Rev. B **57**, 6493 (1998).
[45] T. B. Boykin, N. Kharche, G. Klimeck, and M. Korkusinski, J. Phys.: Condens. Matter **19**, 036203 (2007).
[46] L. Colombo, R. Resta, and S. Baroni, Phys. Rev. B **44**, 5572 (1991).
[47] T. B. Boykin, G. Klimeck, P. von Allmen, S. Lee, and F. Oyafuso, J. Appl. Phys. **97**, 113702 (2005).